Journal of Organometallic Chemistry, 481 (1994) 153–165

Metal π complexes of benzene derivatives

XLIII *. Intramolecular interactions between bis(benzene)chromium and cymantrene units in di- and tri-nuclear species containing PMe_2 spacers, as studied by CV and EPR **

Christoph Elschenbroich, Thomas Isenburg, Bernhard Metz, Andreas Behrendt and Klaus Harms

Fachbereich Chemie der Philipps-Universität, Hans-Meerwein-Strasse, D-35032 Marburg (Germany)

(Received November 18, 1993)

Abstract

Taking advantage of the ability of R_2P-substituted derivatives of bis(benzene)chromium and bis(benzene)vanadium to act as organometallic ligands, we have prepared the di- and tri-nuclear complexes $[(\eta^6\text{-}C_6H_6)(Me_2P\text{-}\eta^6\text{-}C_6H_5)Cr](\eta^5\text{-}MeC_5H_4)(CO)_2Mn)$ (**3**), $\mu\text{-}[(Me_2P\text{-}\eta^6\text{-}C_6H_5)_2Cr](\eta^5\text{-}MeC_5H_4)(CO)_2Mn]_2$ (**7**), $[(Me_2P\text{-}\eta^6\text{-}C_6H_5)_2Cr](\eta^5\text{-}MeC_5H_4)(CO)Mn$ (**9**) and $[(Me_2P\text{-}\eta^6\text{-}C_6H_5)_2V](\eta^5\text{-}MeC_5H_4)(CO)Mn$ (**10**). The structures of **7** and **9** were determined by X-ray diffraction studies. Intermetallic communication in the binuclear complexes is reflected in small shifts of their redox potentials relative to those of the corresponding mononuclear component. Redox splitting for the oxidation of the terminal $MeCpMn(CO)_2$ units of $7^{+\bullet}$ is not resolved. The EPR spectra of $3^{+\bullet}$, $7^{+\bullet}$ and $9^{+\bullet}$ show, in addition to strong ^{53}Cr hyperfine coupling, a small interaction caused by ^{55}Mn. Whereas the monoradical monocations $3^{+\bullet}$, $7^{+\bullet}$ and $9^{+\bullet}$ can be isolated as hexafluorophosphates, the dications $3^{+\bullet+\bullet}$ and $9^{+\bullet+\bullet}$ and the trication $7^{+\bullet+\bullet+\bullet}$, although formed reversibly as indicated by cyclic voltammetry, could not be isolated on a preparative scale. In the case of $9^{+\bullet+\bullet}$ the biradical character was demonstrated by the observation of a $\Delta M_s = 2$ transition in the EPR spectrum. Detailed analysis of the $\Delta M_s = 1$ region was hampered by substantial decomposition of the dication even at low temperature.

Key words: Chromium; Electrochemistry; Vanadium; Electron spin resonance; Manganese; Bis(arene)metals

1. Introduction

One of the more versatile general methods of generating heterobimetallic species involves the use of R_2E-substituted sandwich complexes (E = P or As) as organometallic chelating ligands. This has proved fruitful in the metallocene [2] as well as in the bis(arene)metal [3] series. This approach opens up the possibility of fixing two metals at a well defined intramolecular distance apart in order to study the extent of metal...metal interaction as a function of intermetallic separation and conformational flexibility. There are a number of cases in which dative bonding between two metals has been proposed, eventhough the intermetallic distances considerably exceed the sum of the covalent radii. As the intermetallic separation increases, the value of crystallographically determined distances as a criterion for M...M′ interaction is diminished, and other types of experimental evidence are needed. Among these, the observation of redox splittings in the cyclovoltammetric curves tracing subsequent electron transfer steps and of metal hyperfine splittings in EPR spectra are particularly relevant. The present study addresses the question of whether Cr^I and Mn^I at a distance of ≈ 5 Å show discernible interaction. With this in mind, we have synthesized binuclear complexes composed of bis(benzene)chromium- and (cyclopentadienyl)(carbonyl)manganese

Correspondence to: Prof. Dr. Ch. Elschenbroich.

* For Part, XLII, see ref. 1.

** Herrn Prof. Dr. Helmut Werner zum 60. Geburtstag gewidmet.

0022-328X/94/$7.00
SSDI 0022-328X(94)24588-A

units displaying rigid or dangling structures in order to compare their electrochemical and EPR spectroscopic properties. This investigation complements previous studies that dealt with the properties of early/late transition metal pairs in heterometallic binuclear complexes [4].

2. Results and discussion

2.1. Synthesis and structural characterization

The required complexes **3**, **7**, **9** and **10** were prepared according to Scheme 1 by use of standard reactions. Since in the case of the bifunctional organometallic ligands **4** and **5**, attempted simple photochemical substitution of **2** led to intractable product mixtures, complexes **7**, **9** and **10** were prepared from appropriate precursors in which either one of the Mn coordination sites is taken up by THF or two bear the ligand of them by isoprene, these ligands being radily displaced.

The ^{1}H-, ^{13}C- and ^{31}P NMR data of **3**, **7** and **9** are listed in Table 1. Whereas for the derivatives **3** and **7** free rotation about the C_{arene}–P and P–Mn bonds leads to equivalence of the $P(CH_3)_2$ and the *o*- and *m*-ring protons, respectively, the situation is more subtle in the case of the hetera-[3]chromocyclophane **9**. Here, reversal of the P–Mn–P bridge does not lead to chemical shift equivalence, because, owing to the presence of different substituents Cp′ and CO on the manganese atom, the conformational equilibrium is non-degenerate. Thus, in the slow exchange limit, four $P-CH_3$ signals (CH_{3ax} and CH_{3eq} in different environments) and ten η^6-arene proton signals would be expected. The fact that only two and five resonances, respectively, are observed implies either that only one conformation is populated or that conformational

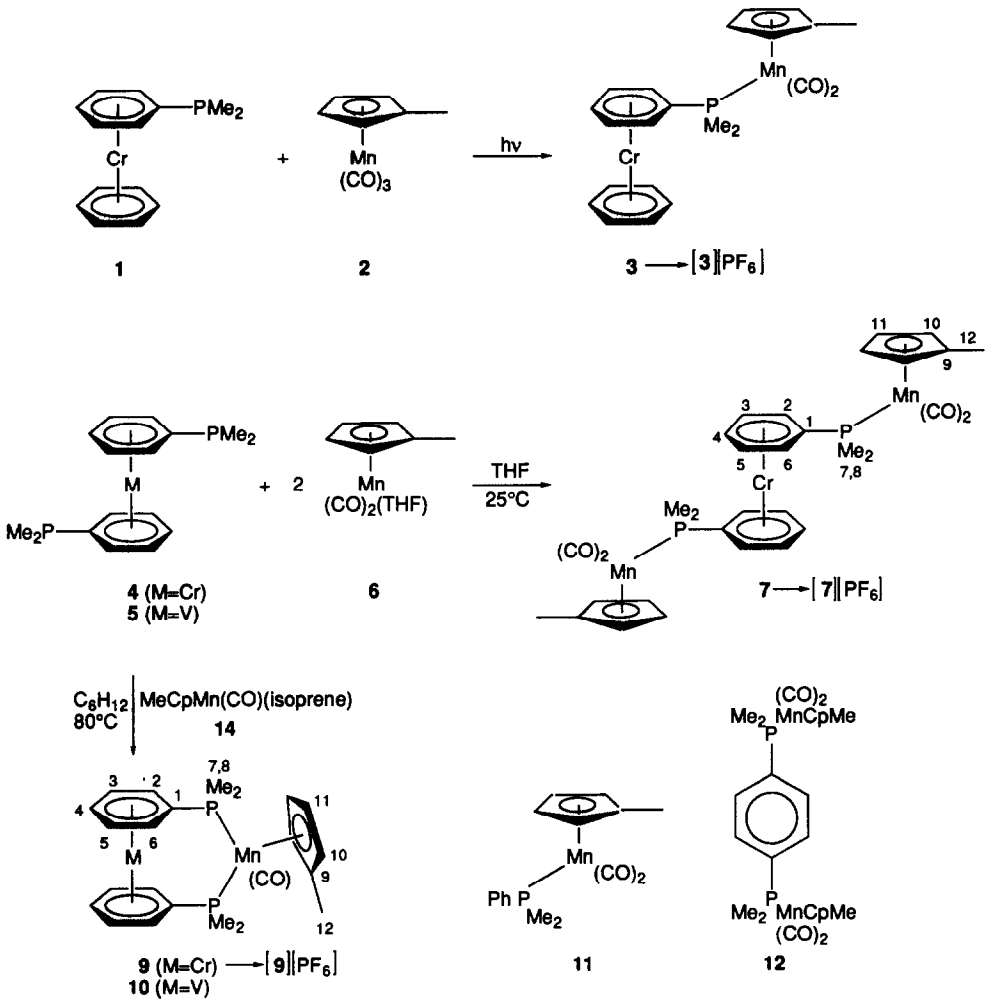

Scheme 1.

TABLE 1. ^{1}H-, $^{13}C\{^{1}H\}$- and $^{31}P\{^{1}H\}$ NMR data (δ (ppm), J (Hz)) for the complexes $MeCpMn(CO)_2(mdmc)$ (3), $[MeCpMn(CO)_2]_2(\mu$-bdmc) (7) and MeCpMn(CO)(bdmc) (9)

	3 [a]	7 [a]	9 [b]		3 [a]	7 [a]	9 [b]
δ(C-1)	90.9d	91.9d	102.8t				
δ(C-2)	75.3d	76.7d	79.6t	δ(H-2)			4.79m
δ(C-3)	73.9d	75.7d	75.2t	δ(H-3)			4.20t
δ(C-4)	73.4s	75.3s	75.0s	δ(H-4)	4.26m	4.36m	4.29t
δ(C-5)			73.6s	δ(H-5)			4.46t
δ(C-6)			76.8t	δ(H-6)			5.70m
δ(C-7)	20.6d	20.9d	27.0t	δ(H-7)	1.54d	1.51d	1.50t
δ(C-8)			21.4t	δ(H-8)			1.53t
δ(C-9)	98.1s	98.4s	91.4s				
δ(C-10)	81.4s	81.4s	78.6s	δ(H-10)	4.01m	4.01m	3.98m
δ(C-11)	82.0s	81.9s	79.2s	δ(H-11)	4.07m	4.08m	4.04m
δ(C-12)	13.8s	13.9s	14.4s	δ(H-12)	1.73s	1.75s	2.27s
$\delta(C_6H_6)$	76.2s			$\delta(C_6H_6)$	4.22m		
				^{2}J(H7,P)	8.2	8.1	3.4
^{1}J(C1,P)	31.8	30.3	18.6	^{2}J(H8,P)			3.5
^{2}J(C2,P)	12.5	12.3	6.4				
^{3}J(C3,P)	6.0	6.0	3.2				
^{1}J(C7,P)	27.8	27.9	12.8				
^{1}J(C8,P)			7.0				
δ(CO)	232.7	232.7	240.1				
$\delta(^{31}P)$	68.6	68.7	61.4				
$\Delta\delta(^{31}P)$	110.8	111.3	104.0				

[a] Benzene-d_6, 25°C. [b] Toluene-d_8, 25°C.

change is fast. Judging from previous experience [5 *] the latter alternative is the more probable, but since in the temperature range $193 < T < 333$ K for **9** no spectral change was observed an unequivocal decision cannot be made.

In the context of the present study, the mutual disposition of the redox active centers Cr^0 and Mn^I is of prime importance. Although solid state structures are not, of course, necessarily the same as those in solution, crystallographic characterization of the open-chain trinuclear complex **7** and the hetera-[3]metallocyclophane **9** nevertheless appeared desirable. The structures of **7** and **9** are shown in Figs. 1 and 2, and the relevant parameters are given in Tables 2 and 3. The most important difference consists of the relative disposition of the chromium and manganese atoms relative to the P(1)C(1)C(4) axis; whereas in **7** these atoms adopt an *anti* disposition, their orientation in **9** is necessarily *cis*. Thus, the Cr ··· Mn distance is smaller in **9** (4.53 Å) than in **7** (5.56 Å). Other noteworthy aspects are the presence of a center of inversion in **7** and the fact that the P–Mn–P interannular link in **9** does not cause bending of the sandwich unit. Presumably, the conformation about the C(1)–P(1) bond found for **7** is also that adopted by the monosubstituted complex **3**.

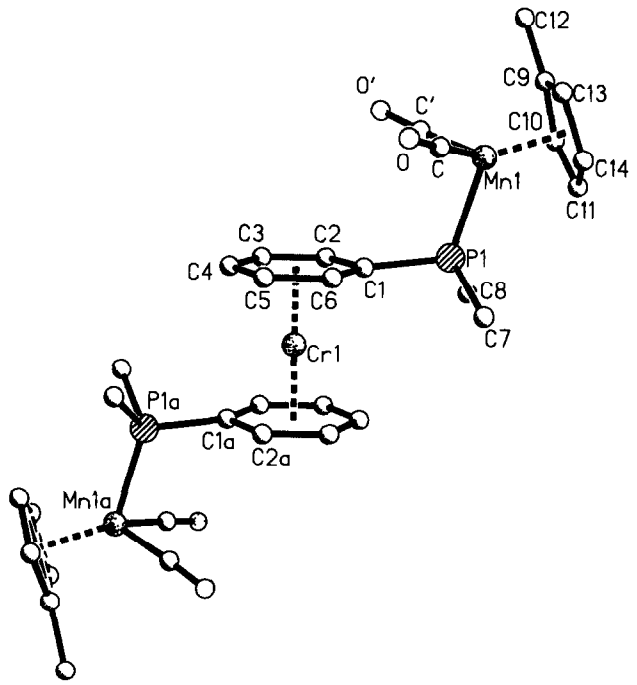

Fig. 1. The molecular structure of compound **7** in the crystal.

* Reference number with asterisk indicates a note in the list of references.

TABLE 2. Selected interatomic distances (Å) and bond angles (°) for **7** [12]

Cr(1)–C(1)	2.168(3)	O–C	1.167(4)	C(9)–C(13)	1.404(5)
Cr(1)–C(2)	2.153(3)	O′–C′	1.170(4)	C(10)–C(11)	1.415(5)
Cr(1)–C(3)	2.150(3)	P(1)–C(1)	1.823(3)	C(11)–C(12)	1.395(6)
Cr(1)–C(4)	2.161(3)	P(1)–C(7)	1.825(3)	C(12)–C(13)	1.418(5)
Cr(1)–C(5)	2.145(5)	P(1)–C(8)	1.816(4)	Cr ··· Mn	5.565(2)
Cr(1)–C(6)	2.146(3)	C(1)–C(2)	1.424(4)		
Mn(1)–C(9)	2.145(3)	C(1)–C(6)	1.423(5)		
Mn(1)–C(10)	2.151(4)	C(2)–C(3)	1.396(5)		
Mn(1)–C(11)	2.141(4)	C(3)–C(4)	1.413(5)		
Mn(1)–C(12)	2.145(4)	C(4)–C(5)	1.398(5)		
Mn(1)–C(13)	2.136(4)	C(5)–C(6)	1.406(4)		
Mn(1)–P(1)	2.225(4)	C(9)–C(10)	1.434(5)		
Mn(1)–C	1.764(4)	C(9)–C(12)	1.508(5)		
Mn(1)–C′	1.757(4)				
C(1)–C(2)–C(3)	121.1(3)	C(7)–P(1)–C(8)	102.6(2)		
C(2)–C(3)–C(4)	120.1(3)	C(8)–P(1)–Mn(1)	116.02(3)		
C(3)–C(4)–C(5)	119.9(3)	C(1)–P(1)–Mn(1)	114.03(11)		
C(4)–C(5)–C(6)	120.2(3)	P(1)–Mn(1)–C	90.07(12)		
C(5)–C(6)–C(1)	120.9(3)	P(1)–Mn(1)–C′	91.66(12)		
C(6)–C(1)–C(2)	117.8(3)	C–Mn(1)–C′	92.2(2)		
C(1)–P(1)–C(7)	104.2(2)				

TABLE 3. Selected interatomic distances (Å) and bond angles (°) for **9** [12]

Cr(1)–C(1)	2.144(6)	Mn–C	1.726(8)	C(1′)–C(6′)	1.418(9)
Cr–C(2)	2.129(6)	C–O	1.185(8)	C(2′)–C(3′)	1.390(9)
Cr–C(3)	2.133(7)	P–C(1′)	1.837(7)	C(3′)–C(4′)	1.399(10)
Cr–C(4)	2.127(7)	P–C(7′)	1.832(8)	C(4′)–C(5′)	1.400(10)
Cr–C(5)	2.134(7)	P–C(8′)	1.804(8)	C(5′)–C(6′)	1.401(10)
Cr–C(6)	2.122(6)	P′–C(1)	1.837(7)	C(9)–C(10)	1.431(12)
Cr–C(1′)	2.152(6)	P′–C(7)	1.842(8)	C(9)–C(12)	1.534(12)
Cr–C(2′)	2.129(7)	P′–C(8)	1.825(7)	C(9)–C(13)	1.389(12)
Cr–C(3′)	2.137(7)	C(1)–C(2)	1.415(9)	C(10)–C(11)	1.403(12)
Cr–C(4′)	2.128(7)	C(1)–C(6)	1.424(8)	C(11)–C(14)	1.363(13)
Cr–C(5′)	2.133(7)	C(2)–C(3)	1.399(9)	C(13)–C(14)	1.384(13)
Cr–C(6′)	2.128(6)	C(3)–C(4)	1.413(10)	Cr ··· Mn	4.530(2)
Mn–C(9)	2.160(8)	C(4)–C(5)	1.371(9)		
Mn–C(10)	2.125(8)	C(5)–C(6)	1.386(9)		
Mn–C(11)	2.102(9)	C(1′)–C(2′)	1.393(9)		
Mn–C(13)	2.159(9)				
Mn–C(14)	2.154(9)				
Mn–P	2.193(8)				
Mn–P′	2.184(2)				
C(1)–C(2)–C(3)	121.5(7)	C(7)–P′–C(8)	118.3(4)		
C(2)–C(3)–C(4)	119.0(7)	C(8)–P′–Mn	118.3(3)		
C(3)–C(4)–C(5)	120.6(7)	C(1)–P′–Mn	121.4(2)		
C(4)–C(5)–C(6)	120.5(6)	P′–Mn–C	93.6(2)		
C(5)–C(6)–C(1)	121.3(7)	C–Mn–P	93.4(2)		
C(6)–C(1)–C(2)	117.0(6)	P–Mn–P′	95.8(2)		
C(1)–P′–C(7)	98.7(3)				
Torsional angles (°)					
C(2)–C(1)–P′–C(8)	10.0(7)				
C(2)–C(1)–P′–C(7)	111.0(6)				
C(1)–P′–Mn–C	−48.7(4)				
C(1)–P′–Mn–P	45.0(3)				

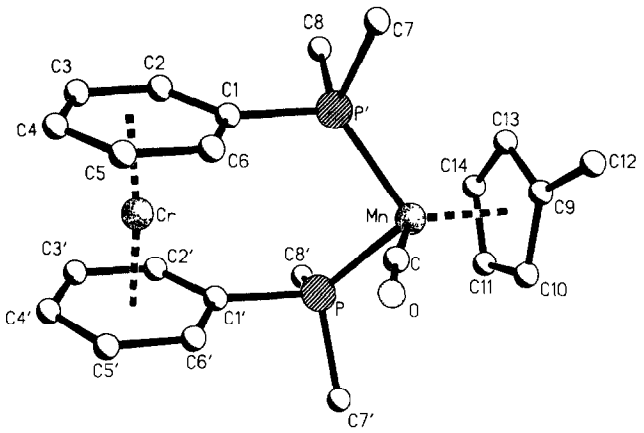

Fig. 2. The molecular structure of compound **9** in the crystal.

2.2. Electrochemical properties

As depicted in Scheme 1, the complexes **3**, **7** and **9** can be oxidized chemically to the corresponding monocations and isolated as stable salts with PF_6^- as the counterion. Since the substrates contain two (**3**, **9**) or three (**7**) redox sites, a cyclovoltammetric study was undertaken. Figure 3 shows the CV traces and the relevant data are listed in Table 4. In all three cases, irreversible reduction is observed near the cathodic border of the medium. The anodic sweep reveals two reversible redox couples with peak-current ratios of 1:1 for **3** and **9** and 1:2 for **7**. This fact, considered together with reference to the redox potentials of the mononuclear units leads to the assignment indicated in Table 4. The initial oxidation of the bis(arene)chromium moiety experiences anodic shifts of +20 and +70 mV upon coordination of one and two $Cp'Mn(CO)_2$ fragments, respectively, to the bridging PMe_2 groups. A shift in the opposite direction of −80 mV is observed when the Cp'Mn(CO) fragment is coordinated to **4** to yield the chelate complex **9**. This illustrates the decisive role of the number of CO ligands in governing the electronic demand of a carbonyl metal fragment [6]. The second redox process involves the cymantrene moiety; relative to the reference species $Cp'Mn(CO)_2(PMe_2Ph)$ (**11**) there are anodic shifts of 30 mV (**3**) and 60 mV (**7**) which are the consequence of the positive charge on chromium in the neighboring sandwich unit. No redox-splitting is discernible for the two Mn^I/Mn^{II} couples present in **7**, which means that the two electron transfer processes proceed virtually independently of each other. This is not very surprising in view of the fact that the complex $[Cp'Mn(CO)_2]_2[1,4\text{-}Me_2PC_6H_4PMe_2]$ (**12**), in which the bis(η^6-arene)chromium unit of **7** is replaced by a phenyl ring, also fails to show a redox-splitting [7]. However, the presence of two $Cp'Mn(CO)_2$ fragments in **7**, compared with just one in **3**, manifests itself in an anodic shift of +30 mV for $E_{1/2}(7^{+/3+})$ compared with $E_{1/2}(3^{+/2+})$. Just as the attachment of $Cp'Mn(CO)_2$ to **1** renders removal of an electron from chromium more difficult, it may also impede ionization of the "opposite" manganese atom in $7^{+\bullet}$. Interestingly, a much more pronounced anodic shift (+220 mV) for the redox couple Mn^I/Mn^{II} is observed when the bis(arene)chromium unit **4** is linked to manganese in a chelating fashion (**9**). Here, the larger effect of the positive charge on chromium on the manganese ionization can be accounted for in terms of the closer proximity of the two metals in **9** than in **3**, and of the presence of two channels for the transmission of electronic effects from chromium to manganese. Conversely, the presence of two electron-accepting CO ligands in **3** and **7** may reduce the propensity of the manganese atoms to respond to electronic perturbation.

For reasons detailed in the following section, we also prepared complex **10**, the vanadium analog of **9**. Its redox behaviour is characterized by quasi-reversibility of the redox couples $V^{+/0}$ and $Mn^{2+/+}$. Just like the chromium complex **4**, its vanadium analog **5** experiences a slight cathodic shift of the redox couple $M^{+/0}$ of the bis(arene)metal unit when the PMe_2 groups are coordinated to the Cp'Mn(CO) fragment.

2.3. Electron paramagnetic resonance

The pronounced separation of the first and second oxidation steps for the complexes **3**, **7** and **9** suggested that, in principle, individual EPR studies of the monoradical cations $3^{+\bullet}$, $7^{+\bullet}$ and $9^{+\bullet}$, the diradical cations $3^{+\bullet+\bullet}$ and $9^{+\bullet+\bullet}$, and the triradical trication $7^{+\bullet+\bullet+\bullet}$ should be possible, provided the various species display sufficient chemical stability. The monocations are easily accessible by air oxidation or oxidation by 4-pyridinecarbaldehyde; their EPR spectra, which are typical for bis(η^6-arene)chromium(d^5) species, are presented in Fig. 4; the parameters are listed in Table 5. The most noteworthy aspect is the resolution of hyperfine coupling to ^{55}Mn in the isotropic EPR spectrum of $9^{+\bullet}$. While in the case of **9** this coupling may be directly observed from the spectrum, for the open complex $3^{+\bullet}$ it is hidden under the broad line. It serves, however, to clarify the initially perplexing observation that a bis(arene)chromium$^{+\bullet}$ radical cation with an odd number of peripheral protons gives rise to an odd number of hyperfine components. As proved by computer simulation, this is a consequence of the $\approx 1:5$ ratio of the magnitudes of a (^{55}Mn, $I = 5/2$) and a (^1H, $I = 1/2$). In the case of the interannularly bridged complex $9^{+\bullet}$ this coupling situation leads to a hyperfine pattern suggesting that there is an even number of principal

components, which is at variance with the presence of an even number of equivalent protons. By contrast, the presence of two manganese nuclei in $7^{+\bullet}$ removes this apparent inconsistency and a hyperfine pattern with a central line of maximum intensity is observed. The analysis of the spectrum of $7^{+\bullet}$ is, however, uncertain, in that hyperfine coupling constants $a(2\ ^{55}Mn)$ of 0.036 and 0.072 mT equally reproduce the experimental trace.

The observation of isotropic hyperfine interaction implies a finite spin density in an s orbital of the coupling nucleus, and therefore the question arises as to the way in which spin density is transferred to manganese. This problem is closely related to that of the interaction that is responsible for isotropic coupling to β-protons in alkyl-substituted derivatives of bis(benzene)chromium radical cations [8]. In the latter

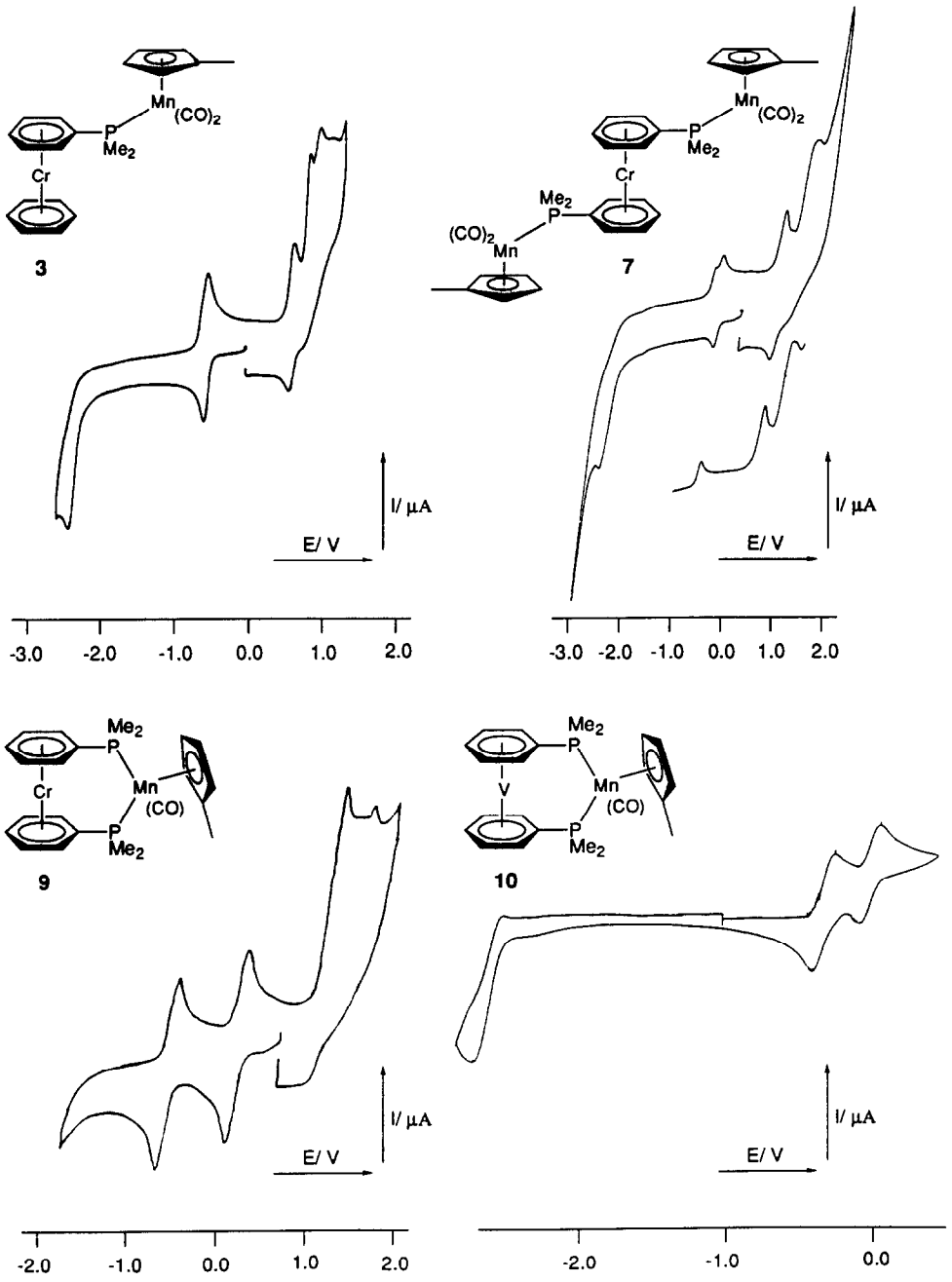

Fig. 3. Cyclovoltammetric curves for the complexes **3**, **7**, **9** and **10** in dimethoxy ethane (0.1 M. Bu_4NClO_4) at glassy carbon *versus* SCE. For temperatures and scan rates see Table 4.

case, it was found necessary to postulate an aggregate mechanism consisting of direct (conformationally independent) spin delocalization $Cr(3d^1_{z^2}) \rightarrow H_\beta(1s)$ and indirect spin polarization $Cr(3d^1_{z^2})/e^4_{2g}(MO)$ followed by (conformationally dependent) hyperconjugation $e^4_{2g} \rightarrow H_\beta(1s)$ (Fig. 5). From the conformational dependence of the coupling constants $a(^1H_\beta)$, it was concluded that the two mechanisms contribute in a 1:3 ratio. While such a dissection will not be attempted here it should be emphasized that the proposed analogy between C–H and P–Mn hyperconjugation with the spin-polarized MO e_{2g} leads to coupling constants $a(^{55}Mn)$ of the correct order of magnitude. Taking the coupling constant $a(^1H_{CH_2})$ as −0.083 mT for the radical cation bis(cyclobuta-η^6-benzene)chromium$^{+\bullet}$ ($\mathbf{13}^{+\bullet}$) to signify that the spin density in the 1s orbital of H_β amounts to $0.083/50.8 = 0.0016$, consideration of the value of a_{iso} = 109.3 mT for an electron localized in a pure Mn 4s orbital [9] and adoption of the s spin density derived for H_β ($\mathbf{13}^{+\bullet}$) for the case of manganese leads to the value a (^{55}Mn) of 0.17 mT, which is somewhat larger than the experimental value. Obviously, P–Mn hyperconjugation is less effective than C–H hyperconjugation, and in the present case this may be due to the greater length of a C–P than of a C–C bond. In view of the limited resolution and the attendant uncertainties in the hyperfine parameters, it would be inappropriate to try to account for the small apparent difference in $a(^{55}Mn)$ for $\mathbf{3}^{+\bullet}$ and $\mathbf{9}^{+\bullet}$.

In bis(η^6-arene)metal(d^5) complexes, the unpaired electron resides in a metal centred orbital of almost exclusively $3d_{z^2}$ character. Since the extension of this orbital and, therefore, the hyperfine coupling to ^{55}Mn, should correlate with charge, we prepared the vanadium complex **10**, which is the neutral, isoelectronic analogue of the radical cation $\mathbf{9}^{+\bullet}$. However, the attachment of a Cp′Mn(CO) unit to the "ligand" **5**, yielding the [3]vanadocyclophane **10**, does not affect the parameter $a(^{51}V)$ and coupling to ^{55}Mn is not resolved. The hyperfine pattern discernible in the indi-

TABLE 4. Cyclovoltammetric data (in dimethoxy ethane containing 0.1 M Bu_4NClO_4 at glassy carbon *versus* SCE) for the organometallic ligands **1**, **4**, **5**, their coordination compounds with $MeCpMn(CO)_{1,2}$ units **3**, **7**, **9**, **10**, and the complexes **11** and **12** for comparison

	T (°C)	E^i_{pc} (0/−1) (V)	$E_{1/2}$ (0/+1) (V)	ΔE_p (mV)	i_{pa}/i_{pc}	n	$E_{1/2}$ (+1/+2, +3) (V)	ΔE (mV)	i_{pa}/i_{pc}	n	E^i_{pa} (V)
1 [a]											
mdmc	25		−0.62 Cr^0–Cr^I	65		1					1.28
4 [a]											
bdmc	25		−0.57 Cr^0–Cr^I	63		1					1.42
5 [a]											
bdmv	−35	−2.52q	−0.27 V^0–V^I	100							
3 [b]											
$(MeCpMn(CO)_2$ (mdmc)	20	−2.63	−0.60r Cr^0–Cr^I	74	0.98	1	0.70r Mn^I–Mn^{II}	90	1.1	1	0.97, 1.12
7 [b]											
$[(MeCp)Mn(CO)_2]_2$ (μ-bdmc)	20	−2.66	−0.50r Cr^0–Cr^I	87	0.99	1	0.73r Mn^I–Mn^{II}	70	0.95	2	1.23i
11 [b]											
$(MeCp)Mn(CO)_2$ (Me_2PhP)	20	−2.59	0.67r Mn^I–Mn^{II}	48	0.98	1					1.16
9 [b]											
(MeCp)Mn(CO) (bdmc)	20	−2.79	−0.65r Cr^0–Cr^I	74	1.00	1	0.05r Mn^I–Mn^{II}	61	1.05	1	0.95, 1.25
10 [a]											
(MeCp)Mn(CO) (bdmv)	−45	−2.68	−0.30q V^0–V^I	140		1	0.02q Mn^I–Mn^{II}	135		1	1.25
12 [b]											
(MeCp)Mn(CO) $(Me_2PhP)_2$	20		−0.17r Mn^I–Mn^{II}	47	1.02	1					0.84, 1.07

i = irreversible, q = quasireversible, r = reversible, n = number of transferred electrons. [a] $v = 100$ mV s^{-1}, [b] $v = 50$ mV s^{-1}.

TABLE 5. EPR data for the species $3^{+\bullet}$, $7^{+\bullet}$, $9^{+\bullet}$ (THF, 20°C) and $\mathbf{10}^{\bullet}$ (toluene, 20°C), hyperfine coupling constants in mT

	$3^{+\bullet}$	$7^{+\bullet}$	$9^{+\bullet}$	$\mathbf{10}^{\bullet}$
$a(^1H_{Ar})$	0.322	0.301	0.332	0.417
$a(^{55}Mn)$	0.075 [a]	(0.070) [b]	0.074 [c]	d
$a(^{53}Cr, ^{51}V)$	1.80	1.81	1.76	6.28
$\langle g \rangle$	1.9870	1.9847	1.9908	1.9904

[a] Inferred from simulation. [b] Analysis ambiguous (see text). [c] Resolved. [d] No spectral evidence.

vidual components of the ^{51}V octet indicates coupling to the arene protons with a value of $a(10\ ^1H)$ in the usual range for bis(benzene)vanadium.

As stated in the section on CV, the second oxidation of **3**, **7** and **9** involves the cymantrene moiety, leading to species which contain $Cr^{I}(d^5)$ and $Mn^{II}(d^5)$ centres. The extent of interaction between these paramagnetic sites should manifest itself in the EPR spectra. It is well known, however, that the bulk preparation of the 17 valence electron cations $Cp'Mn(CO)L_2^+$ as analytically pure salts is fraught with difficulties, solutions of these cations being quite unstable. The dications expected from the oxidation of **9** and **10** were expected to be even less stable, and so we adopted the technique used by Rieger *et al.* [10], which consists of the oxidation with $AgPF_6$ and rapid freezing of the reaction

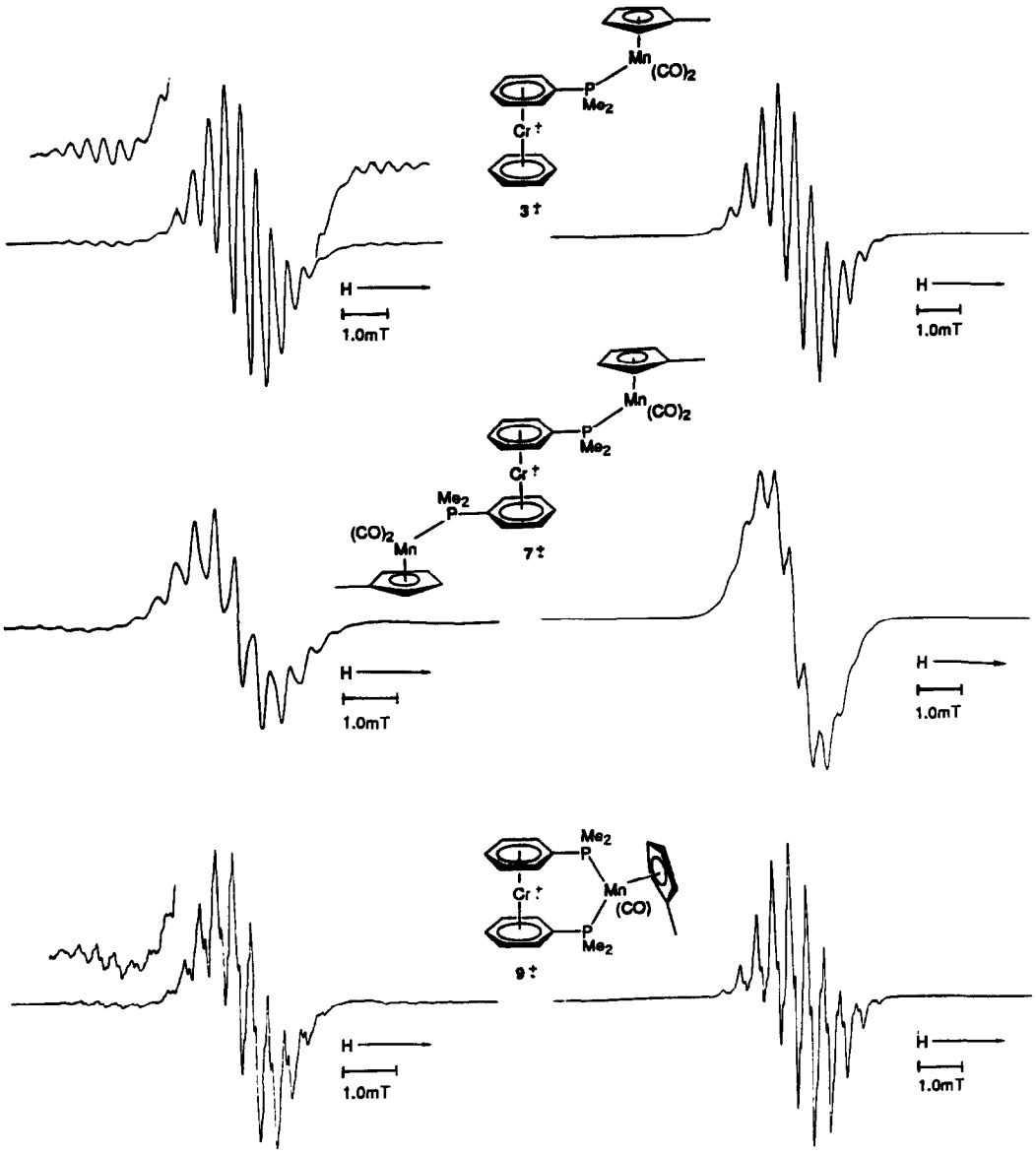

Fig. 4. Isotropic EPR spectra (left) and computer simulations (right) of the radical cations $3^{+\bullet}$, $7^{+\bullet}$ and $9^{+\bullet}$. For conditions and parameters, see Table 5.

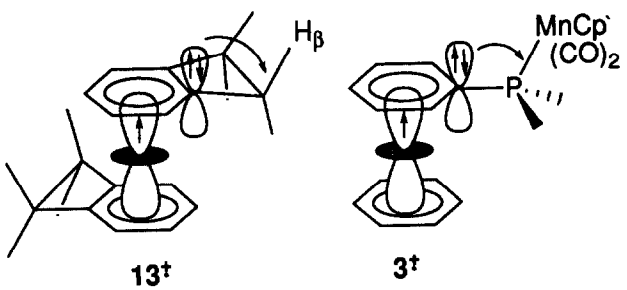

Fig. 5. The contribution of the spin polarization mechanism to the generation of spin density at nuclei in β-position to an η^6-arene. The electron pair in the p_z orbital of the *ipso* carbon atom only serves to illustrate the nature of the process, its density at this position (< 1) is governed by the respective coefficient in the molecular orbital e_{2g}.

product. In this fashion, oxidation of **9** leads to the EPR spectrum in a frozen solution that is shown in Fig. 6. Whereas the biradical nature of $9^{+\bullet+\bullet}$ is proved by the observation of a fairly intense half-field signal ($\Delta M_s = 2$), only tentative conclusions can be drawn from the $\Delta M_s = 1$ region, spectral resolution being poor. The central part points to the presence of mono-radical species stemming from decompositon of the binuclear complex **9**. If the distance between the two outermost peaks is taken to define the zero-field splitting 2D, adoption of the point-dipole approximation and use of the parameter $D = 0.056$ cm^{-1} in the relationship $R = (0.650\ g^2/D)^{1/3}$ Å [11] results in an inter-spin distance of 3.60 Å, which is considerably shorter

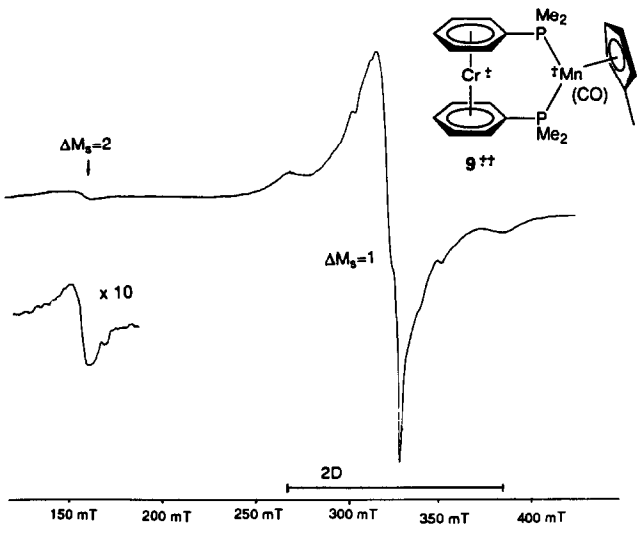

Fig. 6. EPR spectrum of the product obtained in the oxidation of **7** with $AgPF_6$ (rigid solution in THF, 140 K), presumably the species $7^{+\bullet+\bullet}$.

than the intermetallic distance Cr ··· Mn = 4.53 Å derived from a X-ray diffraction study on **9**. Apparently, spin–spin interaction of the two unpaired electrons is not purely dipolar, and a mechanism related to that responsible for the observation of ^{55}Mn hyperfine splitting in the spectrum of $9^{+\bullet}$ may result in the seemingly a shorter intermetallic distance in $9^{+\bullet+\bullet}$. In any case, upon melting the frozen solution of $9^{+\bullet+\bullet}$, EPR signals characteristic of disubstituted bis(arene)chromium$^{+\bullet}$ cations and for solvated Mn^{2+} ions appear. We are thus looking for other metal combinations which should lead to more stable biradical species so that we may study heteronuclear metal–metal interaction by means of EPR.

3. Experimental section

All manipulations were carried with exclusion of air under dinitrogen or argon (CV). Physical measurements were performed with the equipment specified previously [12].

3.1. (η^4-2-Methyl-1,3-butadiene)(η^5-methylcyclopentadienyl)(carbonyl)manganese (14)

A solution of (methylcyclopentadienyl)(tricarbonyl) manganese (**2**) (0.3 ml, 2 mmol) and 2-methyl-1,3-butadiene (5.0 ml, 50 mmol) in 200 ml of cyclohexane was irradiated with a low pressure mercury lamp for 2 h at ambient temperature. The colour changed from yellow to red. The solution was reduced to 50 ml, filtered over Celite and freed from the solvent. Further purification was carried out by chromatography on Al_2O_3 (1% H_2O, elution with toluene/n-hexane, 4:1, column 3 cm × 15 cm). In this way, **14** was obtained as red oil (210 mg, 0.9 mmol, 45%). MS(EI): *m/e* (rel. int.) 230 (4%, M^+), 202 (35%, $M^+ - CO$), 134 (100%, $M^+ - CO$ – isoprene), 55 (31%, Mn^+). MS(HR) for $C_{12}H_{15}MnO$: *m/e* (M^+) calc. 230.05034, found: 230.05076. IR (THF): ν(CO) 1930s cm^{-1}.

3.2. [(Dimethylphosphano-η^6-benzene)(η^6-benzene)chromium](η^5-methylcyclopentadienyl)(dicarbonyl)manganese (3)

A solution of $MeCpMn(CO)_3$ (**2**) (0.50 g, 2.3 mmol) and (Me_2P-η^6-C_6H_5)(η^6-C_6H_6)Cr (**1**) [3c] (0.68 g, 2.5 mmol) was irradiated at ambient temperature for 3 h while being purged with N_2. Removal of the solvent in *vacuo* left a reddish-brown oil, which was taken up in 20 ml of boiling petroleum ether. The solution was filtered, and on cooling gave 150 mg (0.33 mmol, 13.2%) of **3** as brown needles. Anal. Found: C, 57.63; H, 5.25. $C_{22}H_{24}CrMnO_2P$ calc.: C, 57.65; H 5.25%. MS (EI): *m/e* (rel. int.) 458 (33.2, M^+), 380 (19.5, $M^+ - C_6H_6$),

324 (19.9, $M^+ - C_6H_6 - 2CO$), 272 (92.0, $M^+ - C_6H_6 - 2CO - Cr$), 269 (100, $Cp'CrMe_2PC_6H_5^+$), 190 (61.8, $Me_2PC_6H_5Cr^+$), 138 (73.1, $Me_2PC_6H_5^+$), 55 (61.3, Mn^+), 52 (94.2, Cr^+). IR (THF): ν(CO) 1921, 1857 cm^{-1}.

In order to isolate the radical cation $3^{+\bullet}$ as a stable salt, a solution of **3** in toluene was treated with a saturated aqueous solution of NH_4PF_6 and 4-pyridinecarbaldehyde was added as an oxidizing agent to give **3**(PF_6) in almost quantitative yield. Anal. Found: C, 43.24; H, 5.09. $C_{22}H_{24}CrF_6MnO_2P_2$ calc.: C, 43.48; H, 4.60%.

3.3. μ-[Bis(dimethylphosphano-η^6-benzene)chromium] bis[(η^5-methylcyclopentadienyl)(dicarbonyl)manganese] (7)

A solution of $MeCpMn(CO)_3$ (**2**) (0.6 ml, 4.0 mmol) in 200 ml of THF was irradiated at ambient temperature for 5 h causing the solution to turn red. A solution of (Me_2P-η^6-$C_6H_5)_2Cr$ (**4**) [3c] (0.56 g, 1.7 mmol) in 30 ml of THF was added, and stirring at room temperature was continued for 16 h. Removal of the solvent *in vacuo* left a reddish-brown oil, and recrystallization from 15 ml of n-octane gave 220 mg (0.31 mmol, 18.2%) of **7** as brown needles. Anal. Found: C. 53.67; H, 5.27. $C_{32}H_{36}CrMn_2O_4P_2$ calc.; C, 54.24; H, 5.12%. MS (EI): *m/e* (rel. int.) 708 (58.0, M^+), 652 (11.8, $M^+ - 2CO$), 518 (45.5, $M^+ - Cp'Mn(CO)_2$), 462 (27.8, $M^+ - 2CO\text{-}Cp'Mn(CO)_2$), 380 (65.1, $Cp'Mn(CO)_2PMe_2C_6H_5Cr^+$), 328 (71.5, $(Me_2PC_6H_5)_2Cr^+$), 324 (62.0, $Cp'MnPMe_2C_6H_5Cr^+$), 272 (89.5, $Cp'MnMe_2PC_6H_5^+$), 269 (100, $Cp'CrMe_2PC_6H_5^+$), 190 (69.0, $Me_2PC_6H_5Cr^+$), 138 (74.5, $Me_2PC_6H_5^+$), 55 (66.3, Mn^+), 52 (68.3 Cr^+). IR (THF): ν 1921, 1857 cm^{-1}.

The salt **7**(PF_6) was obtained by a procedure analogous to that used for the preparation of **3** (PF_6). Anal.

TABLE 6. Crystallographic data for **7** and **9**

	9	**7**
Empirical formula	$(C_{23}H_{29}CrMnOP_2)(C_{0.5}H_{1.17})$	$C_{32}H_{36}CrMn_2O_4P_2$
Formula weight	497.52	708.43
Temperature (K)	190(2)	190(2)
Wavelength (Å)	0.71073	0.71073
Crystal system	Rhombohedral	Monoclinic
Space group	$R\bar{3}$	$P2_1/c$
Unit cell dimensions		
a (Å)	38.401(8)	14.171(3)
b (Å)	38.401(8)	8.4070(10)
c (Å)	8.255(3)	13.671(3)
α (°)	90	90
β (°)	90	109.44(2)
γ (°)	120	90
Volume (Å^3)	10542(5)	1535.9(5)
z	18	2
Density (calculated (Mg m^{-3})	1.411	1.532
Absorption coefficient (mm^{-1})	1.151	1.297
F(000)	4647	728
Crystal size (mm^3)	0.3 × 0.2 × 0.1	0.25 × 0.15 × 0.15
θ range for data collection (°)	2.12 to 23.56	1.52 to 27.52
Index ranges	$0 \le h \le 37, 0 \le k \le 37, -9 \le l \le 9$	$-18 \le h \le 17, -10 \le k \le 1, -1 \le l \le 17$
Reflections collected	3617	3908
Independent reflections	3444 (R_{int} = 0.0949)	3306 (R_{int} = 0.0373)
Absorption correction	Semi-empirical from ψ-scans	
Max. and min. transmission	0.899 and 0.741	
Refinement method	Full-matrix least-squares on F^2	Full-matrix least squares on F^2
Data/restraints/parameters	3443/0/259	3305/0/223
Goodness-of-fit on F^2	0.820	0.796
Final *R* indices [$I > 2\sigma(I)$]	*R*1 = 0.0533, *wR*2 = 0.1142	*R*1 = 0.0406, *wR*2 = 0.0626
R indices (all data)	*R*1 = 0.1240, *wR*2 = 0.1376	*R*1 = 0.0852, *wR*2 = 0.1395
Largest diff. peak and hole (e Å^{-3})	0.616 and −0.373	0.341 and −0.302

Found: C. 45.32; H, 4.36. $C_{32}H_{36}CrF_6Mn_2O_4P_3$ calc. C, 45.02; H, 4.25%.

3.4. [Bis(dimethylphosphano-η^6-benzene)chromium](η⁵-methylcyclopentadienyl)(carbonyl)manganese (9)

A solution of **14** (0.50 g, 2.2 mmol) and **4** (0.60 g, 1.8 mmol) in cyclohexane (50 ml) was heated under reflux for 4 h. The end of the reaction was indicated by the replacement of the IR absorption at 1930 by one at 1836 cm^{-1}. After removal of the solvent, the brown residue was subjected to chromatography (Al_2O_3, 1% H_2O column 3 × 15 cm). Elution with toluene/n-hexane (4:1) gave a red band of (**12**), followed by a brown band which contained the product **9**. The latter was recrystallized from 20 ml of n-hexane to yield 120 mg (0.24 mmol, 10.5%) of **9** as golden yellow needles. Anal. Found: C, 56.63; H, 6.14. $C_{23}H_{29}CrMnOP_2$ calc.: C, 56.34; H, 5.96%. MS (EI): *m/e* (rel. int.) 490 (19.7, M^+) 462 (27.6, $M^+ - CO$), 328 (23.0, $(Me_2PC_6H_5)_2Cr^+$), 272 (49.3, $M^+ - CO - Me_2PC_6H_5Cr$), 269 (69.9, $Cp'CrMe_2PC_6H_5^+$), 190 (30.7, $Me_2PC_6H_5Cr^+$), 134 (22.0, $Me_2PC_6H_5^+$), 55 (23.0, Mn^+), 52 (100, Cr^+). IR (THF): ν(CO) 1816 cm^{-1}.

The salt **9** (PF_6) was prepared as described above. Anal. Found: C, 43.24; H, 5.09. $C_{23}H_{29}CrF_6MnOP_3$ calc.: C, 43.48; H, 4.60%.

TABLE 7. Atomic coordinates (×10⁴) and equivalent isotropic displacement parameters (Å² × 10³) for 7

	x	y	z	U_{eq} [a]
Cr(1)	5000	5000	5000	24(1)
Mn(1)	1841(1)	708(1)	4180(1)	27(1)
P(1)	2868(1)	2283(1)	3696(1)	27(1)
O	1377(2)	3299(3)	5380(2)	49(1)
O'	3459(2)	−488(3)	5978(2)	55(1)
C(1)	3778(2)	3331(4)	4766(2)	24(1)
C(2)	4696(3)	2603(4)	5363(3)	30(1)
C(3)	5333(3)	3325(5)	6259(3)	36(1)
C(4)	5065(3)	4793(5)	6596(3)	36(1)
C(5)	4173(3)	5540(4)	6018(3)	31(1)
C(6)	3530(2)	4818(4)	5114(3)	28(1)
C(7)	2247(2)	3858(4)	2794(2)	34(1)
C(8)	3628(2)	1317(4)	3031(3)	42(1)
C(9)	1056(3)	−1510(4)	4018(3)	34(1)
C(13)	364(3)	−255(5)	3747(3)	38(1)
C(12)	474(3)	580(5)	2890(3)	43(1)
C(11)	1233(3)	−178(5)	2628(3)	45(1)
C(10)	1608(3)	−1472(5)	3308(3)	40(1)
C(12)	1146(3)	−2724(4)	4857(3)	50(1)
C	1572(2)	2286(4)	4896(3)	34(1)
C'	2826(3)	25(4)	5260(3)	34(1)

[a] U_{eq} is defined as one-third of the trace of the orthogonalized U_{ij} tensor.

3.5. [Bis(dimethylphosphano-η^6-benzene)vanadium](η⁵-methylcyclopentadienyl)(carbonyl)manganese (10)

The procedure for **10** was similar to that used for **9**. Anal. Found: C, 55.63; H, 5.92. $C_{23}H_{29}MnOP_2V$ calc.: C, 56.45; H, 5.97%. MS (HR): *m/e* (M^+) calc. 489.05137, found 489.05143. MS (EI): *m/e* (rel. int.) 489 (36.4%, M^+), 461 (87.2, $M^+ - CO$), 327 (100, $(Me_2PC_6H_5)_2V^+$), 272 (23.8, $M^+ - CO - Me_2PC_6H_5V$), 138 (20.0, $Me_2PC_6H_5^+$) 55 (17.9, Mn^+) 51 (10.3, V^+). IR (THF): ν(CO) 1821 cm^{-1}.

3.6. X-Ray structure determination of compounds 7 and 9

Crystal data and other parameters related to the structure determination are listed in Table 6. Atomic coordinates and equivalent isotropic displacement parameters are listed in Tables 7 and 8; the most significant bond lengths and angles are given in Tables 2 and 3 [13 *].

3.6.1. Data collection and reduction for 7

The crystal (0.25 × 0.15 × 0.15 mm^3) was mounted in inert oil on a glass fibre which was placed in the cold gas stream of the diffractometer (Siemens P4 with LT-2 low temperature attachment). Data were collected to $2\theta = 55°$ with monochromated Mo-Kα radiation. Cell constants were refined from diffractometer angles of 30 reflections with $2\theta > 20°$. Of 3908 reflections, 3306 were unique ($R_{int} = 0.0373$).

3.6.2. Structure solution and refinement for 7

The structure was solved by the heavy-atom method. Non-hydrogen atoms were refined anisotropically, methyl hydrogens were included using a riding model, the other hydrogens were refined isotropically. Refinement on F^2 (program SHELXL-93) proceeded to $wR2 = 0.1414$ for all data with only reflection 1 0 0 omitted (conventional $R = 0.0407$ for 1892 reflections $> 2\sigma(I)$). The weighting scheme was $w^{-1} = \sigma^2(F_o^2) + 0.0189P^2$ with $P = F_o^2 + 2F_c^2)/3$; goodness-of-fit on $F^2 = 0.799$; max. $\Delta\rho = 0.34$ e $Å^{-3}$.

3.6.3. Data collection and reduction for 9

The crystal (0.3 × 0.2 × 0.1 mm^3) was mounted in inert oil on a glass fibre and transferred to the cold gas stream of the diffractometer (Siemens R3 with LT-2 low temperature attachment). Data were collected to $2\theta = 47°$ with monochromated Mo-Kα radiation. Cell constants were refined from diffractometer angles of 30 reflections with $2\theta > 20°$. Of 3617 reflections, 3444 were unique ($R_{int} = 0.0949$). An empirical absorption correction was applied using the XEMP in the program system Siemens SHELXTL PLUS.

TABLE 8. Atomic coordinates ($\times 10^4$) and equivalent isotropic displacement parameters ($Å^2 \times 10^3$) for **9**

	x	y	z	U_{eq} [a]
Cr	1594(1)	626(1)	7371(1)	41(1)
Mn	2818(1)	731(1)	7869(1)	47(1)
P'	2256(1)	201(1)	7089(2)	50(1)
P	2535(1)	959(1)	9545(2)	59(1)
C(1)	1810(2)	237(2)	6565(8)	43(2)
C(2)	1427(2)	8(2)	7290(9)	53(2)
C(3)	1100(2)	47(2)	6806(10)	59(2)
C(4)	1153(2)	319(2)	5551(9)	59(2)
C(5)	1519(2)	541(2)	4813(9)	59(2)
C(6)	1846(2)	506(2)	5303(7)	38(2)
C(7)	2301(3)	−28(3)	5200(11)	93(3)
C(8)	2039(3)	−244(2)	8381(12)	106(4)
C(9)	3342(3)	716(4)	7010(12)	81(3)
C(10)	3455(2)	1048(3)	8082(15)	83(3)
C(11)	3277(3)	884(4)	9583(13)	91(3)
C(12)	3466(3)	724(3)	5239(13)	133(4)
C(13)	3105(3)	370(3)	7906(16)	85(3)
C(14)	3072(3)	475(4)	9479(17)	99(4)
C(1')	2069(2)	963(2)	9080(8)	47(2)
C(2')	1707(2)	735(2)	9898(9)	60(2)
C(3')	1358(2)	741(3)	9518(10)	64(2)
C(4')	1371(3)	996(3)	8278(12)	71(3)
C(5')	1731(3)	1237(2)	7442(10)	66(2)
C(6')	2077(2)	1218(2)	7821(9)	53(2)
C(7')	2851(2)	1492(3)	10054(12)	127(5)
C(8')	2412(3)	746(4)	11553(10)	136(5)
C	2819(2)	1024(2)	6282(9)	49(2)
O	2848(2)	1238(2)	5193(6)	73(2)
C(101)	−36	60	4099	81(10)
C(102)	134	−5	2496	81(10)
C(103)	−88	33	993	81(10)
C(10A)	140	−39	5610	81(10)
C(10B)	110	8	−611	81(10)
C(10C)	−20	42	7211	81(10)

[a] U_{eq} is defined as one-third of the trace of the orthogonalized U_{ij} tensor.

3.6.4. Structure solution and refinement for 9

The structure was solved by the heavy-atom method (SHELXTL PLUS). Non-hydrogen atoms were refined anisotropically, hydrogens were included using a riding model. Disordered solvent was assumed to be hexane and was refined as an idealized rigid group with fixed isotropic temperature parameters so that 1.5 solvent molecules were in the unit cell. Refinement of F^2 (program SHELXL-93) proceeded to $wR2 = 0.1376$ for all data (conventional $R = 0.0533$ for 1702 reflections $> 2\sigma(I)$). The weighting scheme was $w^{-1} = \sigma^2(F_o^2) + 0.0641P^2$ with $P = (F_o^2 + 2F_c^2)/3$; goodness-of-fit on $F^2 = 0.820$; max. $\Delta\rho = 0.62$ e Å^{-3}.

Acknowledgements

This work was supported by the Deutsche Forschungsgmeinschaft and the Fonds der Chemischen Industrie. A.B. gratefully acknowledges the award of a research scholarship in the Graduiertenkolleg Metallorganische Chemie.

References and notes

1 Ch. Elschenbroich, A. Bretschneider-Hurley, J. Hurley, W. Massa, S. Wocadlo and J. Pebler, *Inorg. Chem., 32* (1993) 5421.

2 (a) J.J. Bishop, A. Davison, M.L. Katchar, D.W. Lichtenberg, R.E. Merrill and J.C. Smart, *J. Organomet. Chem., 27* (1971) 241; J.J. Bishop and A. Davison, *Inorg. Chem., 10* (1971) 826, 832; (b) D. Seyferth and H.P. Withers, Jr., *Organometallics, 1* (1982) 1275; (c) P.H. Demerseman, P.H. Dixneuf, J. Donglade and R. Mercier, *Inorg. Chem., 21* (1982) 3942; (d) W.R. Cullen, T.J. Kim, F.W.B. Einstein and T. Jones, *Organometallics, 2* (1983) 714; (e) T. Hayashi, M. Konishi, J. Kobori, M. Kumada, T. Higuchi and K. Hirotsu, *J. Am. Chem. Soc., 106* (1984) 158; (f) F.R. Butler, W.R. Cullen, T.-J. Kim, S.J. Rettig and J. Trotter, *Organometallics, 4* (1985) 972. (g) W. Tikkanen, Y. Fujita and J.L. Petersen, *Organometallics, 5* (1985) 888; (h) M. Rausch, M. Ogasa, M.A. Ayers, R. Rogers and A. Rollins, *Organometallics, 10* (1991) 2481; (i) T.-J. Kim, S.-C. Kwon; Y.-H. Kim, N.H. Heo, M.M. Teuter and A. Yamano, *J. Organomet. Chem., 426* (1992) 71; (j) G. Pilloni and B. Logato, *Inorg. Chim. Acta, 208* (1993) 17; (k) M.I. Bruce, I.R. Butler, W.R. Cullen, D.R. Konstantonis, M.R. Snow and E.R.T. Tieking, *Aust. J. Chem., 41* (1988) 963; M. Sato and M. Sekino, *J. Organomet. Chem., 444* (1993) 185; (l) S. Onaka H. Furuta and S. Takagi, *Angew. Chem., 105* (1993) 105; *Angew. Chem., Int. Ed. Engl., 32* (1993) 87.

3 (a) Ch. Elschenbroich and F. Stohler, *Angew. Chem., 87* (1975) 198; *Angew. Chem., Int. Ed. Engl., 14* (1975) 174; (b) R. Faggiani, N. Hao, C.J.L. Lock, B.G. Sayer and M.J. McGlinchey, *Organometallics, 2* (1983) 96; (c) Ch. Elschenbroich, G. Heikenfeld, M. Wünsch, W. Massa and G. Baum, *Angew. Chem., 100* (1988) 397; *Angew. Chem., Int. Ed. Engl., 27* (1988) 414. (d) Ch. Elschenbroich, J. Sebbach, B. Metz and G. Heikenfeld, *J. Organomet. Chem., 426* (1992) 173.

4 (a) M. Clemance, R.M.G. Roberts and J. Silver, *J. Organomet. Chem., 243* (1983) 461; (b) S. Akabori, T. Kunnagai, T. Shirahige, S. Sato, K. Kawazoe, C. Tamura and M. Sato, *Organometallics, 6* (1987) 526; (c) M. Sato, M. Sekino and S. Akabori, *J. Organomet. Chem., 344* (1988) C31; (d) D.W. Stephan, *Coord. Chem. Rev., 95* (1989) 41; (e) R. Rousseau and D.W. Stephan, *Organometallics, 10* (1991) 3399 and refs. therein; (f) T.T. Nadasdi and D.W. Stephan, *Organometallics, 11* (1992) 116.

5 (a) Fluxionality of the interannular bridge $-AsPh_2-M(CO)_4-AsPh_2-$ (M = Cr, Mo, W) in [3]ferrocenophanes has been observed as early as 1971 [2a], (b) the stereodynamics of related [3]ferrocenophane complexes with S-, Se- and Te-containing interannular bridges have been studied in great detail by Abel *et al.*; E. Abel, S.K. Bhargava and K.G. Orell, *Prog. Inorg. Chem., 32* (1984); (c) the flexibility of interannular bridges $-SeMe-Cr(CO)_4-SeMe-$ at bis(benzene)chromium has also been investigated: Ch. Elschenbroich, H. Burdorf, D. Mahrwald and B. Metz, *Z. Naturforsch., 47b* (1992) 1157.

6 N.G. Connelly and M.D. Kitchen, *J. Chem. Soc., Dalton Trans., 931* (1977).

7 R. Gross-Lannert, W. Kaim, U. Lechner, E. Roth and C. Volger, *Z. Anorg. Allg. Chem., 579* (1989) 47.

8 Ch. Elschenbroich, J. Koch, J. Schneider and B. Spangenberg, *J. Organomet. Chem., 317* (1986) 41.

9 B.A. Goodman and J.B. Raynor, *Adv. Inorg. Chem. Radiochem., 13* (1970) 135.

10 R.D. Pike, A.L. Rieger and P.H. Rieger, *J. Chem. Soc., Faraday Trans.*, I *85* (1989) 3913.
11 N.D. Chasteen and R.L. Belford, *Inorg. Chem., 9* (1970) 169.
12 Ch. Elschenbroich, M. Nowotny, J. Kroker, A. Behrendt, W. Massa and S. Wocadlo, *J. Organomet. Chem., 459* (1993) 157.
13 Further details of the crystal structure investigation are available on request from the Fachinformationszentrum Karlsruhe, Gesellschaft für wissenschaftlich-technische Information mbH, D-76344 Eggenstein-Leopoldshafen (Germany) on quoting the depository numbers CSD-400422 (**7**), CSD-400417 (**9**), the names of the authors, and the journal citation.